Effects of disorder on conductance oscillations in semiconductor-superconductor junctions in a magnetic field

Yasuhiro Asano* and Takashi Yuito
Department of Applied Physics, Hokkaido University, Sapporo 060-8628, Japan
(Received 17 February 2000; revised manuscript received 25 April 2000)

We study the effects of disorder on magnetoconductance oscillations in semiconductor-superconductor junctions. These conductance oscillations were predicted by recent several theoretical works in ballistic junctions, however, have never been observed yet in experiments. We find that the disorder near the junction suppresses the conductance oscillations. From the numerical results, we derive a condition that must be satisfied to find the conductance oscillations in experiments.

I. INTRODUCTION

In recent years, a study of small hybrid systems consisting of a superconductor in contact with a semiconductor has attracted much attention.[1–4] The unusual reflection from the normal metal-superconductor interface, known as the Andreev reflection,[5] characterizes the transport properties in semiconductor/superconductor (Sm-*S*) systems.[6] In experiments, *S*-Sm-*S* junctions are realized in the strong magnetic fields by using a superconductor with high-critical magnetic field.[7,8] The Andreev reflection at each Sm-*S* interface is the source of the Josephson current that is carried by the edge states in high-magnetic fields.[9,10] These investigations bridge the quantum Hall effect and the Andreev reflection.

The magnetoconductance oscillations in semiconductor/superconductor (Sm-*S*) junctions are a consequence of the Andreev reflection of a quasiparticle under the magnetic field. These oscillations were first found in a numerical simulation.[11] In previous papers, we proposed the mechanism of the conductance oscillations and concluded that the Aharonov-Bohm type interference effect is responsible for the oscillations.[12,13] Within a phenomenological argument, we explained the amplitude, the period, and the phase shift of the conductance oscillations. A recent microscopic calculation showed the conductance oscillations,[14] which are similar to those in the numerical simulation.[11] Unfortunately the conductance oscillations have never been observed yet in experiments. In the theoretical works, it is assumed that the Sm-*S* junctions are free from any disorder and that the magnetic field in the superconductor is perfectly excluded by the Meissner effect. If the proposed mechanism of the oscillations is correct,[12] the conductance oscillations are sensitive to disorder near the Sm-*S* interface. In addition to this, it is also predicted that the conductance oscillations might be smeared by the magnetic field that penetrates into the superconductor.[13] The effects of disorder on the conductance oscillations should be studied theoretically to find the oscillations in experiments. So far, the effects of the impurity scattering in the semiconductor was briefly discussed in a numerical simulation.[15]

There are two purposes in this paper. One of them is to check the validity of the proposed mechanism of the conductance oscillations.[12] Second purpose is to discuss a possibility of the conductance oscillations finding in experiments. For these purposes, we perform a numerical simulation by using the recursive Green's-function method[16,17] and calculate the zero-bias conductance based on the Takane-Ebisawa formula.[18] The numerical results show that the conductance oscillations disappear when the elastic mean-free path in the semiconductor is smaller than the diameter of the classical cyclotron orbit of a quasiparticle. The effects of the rough Sm-*S* interface on the conductance oscillations are studied in terms of the specularity of the interface. We show that the specular reflection at the Sm-*S* interface is an important ingredient for the conductance oscillations. These calculated results are consistent with the prediction in the phenomenological theory.[12]

This paper is organized as follows. In Sec. II, we briefly survey the mechanism of the magnetoconductance oscillations in Sm-*S* junction. The effects of the impurity scattering in the semiconductor and those of the rough interface on the conductance oscillations are discussed in Sec. III. In Sec. IV, a possibility of the conductance oscillations in experiments is argued. The conclusion is given in Sec. V.

II. MECHANISM OF THE CONDUCTANCE OSCILLATIONS

Let us consider a situation where both the normal and Andreev reflection processes exist at the Sm-*S* interface, and the superconductor is one of the type I. In Fig. 1, we schematically illustrate the classical trajectories of a quasiparticle near the Sm-*S* interface in a magnetic field, where the hatched area denotes the superconductor and the width of the Sm-*S* junction is *W*. We assume that the system is free from any disorder and that the magnetic field is perfectly excluded from the superconductor. In Fig. 1(a), the magnetic field is sufficiently weak and an incident electronlike quasiparticle is reflected once at the Sm-*S* interface. In the presence of the magnetic field, the Andreev-reflected holelike quasiparticle does not trace the trajectory of the incident quasiparticle. The quasiparticle in the electron branch and that in the hole branch skip along the Sm-*S* interface in the same direction. This is because the signs of the charge in the two branches are opposite to each other. At the same time, the signs of the effective mass in the two excitations are opposite to each

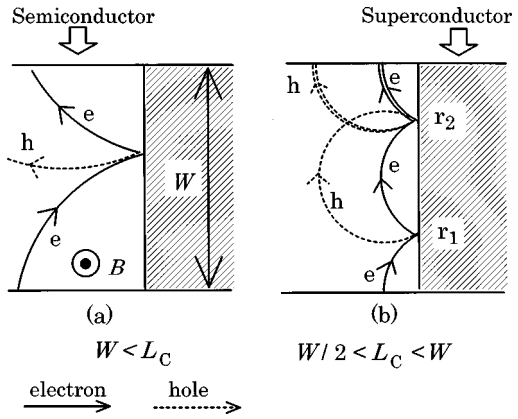

FIG. 1. The classical trajectories of a quasiparticle in magnetic field are depicted. The hatched area is the superconductor. The solid (broken) curves are the cyclotron orbits of a quasiparticle in the electron (hole) branch. The width of the junction is W and L_C is the diameter of the classical cyclotron motion of a quasiparticle.

other. The diameter of the classical cyclotron orbit is given by

$$L_C=\frac{4}{k_F}\frac{\mu_N}{\hbar\omega_c}, \tag{2.1}$$

where k_F, μ_N, and $\omega_c=eB/m^*c$ are the Fermi wave number, the Fermi energy, and the cyclotron frequency in the two-dimensional electron gas (2DEG) on the semiconductor, respectively.

In Fig. 1(b), the magnetic field is slightly stronger than that in Fig. 1(a), where the incident quasiparticle is reflected twice at the Sm-S interface. The incident quasiparticle is either reflected into the electron or the hole branches at $\mathbf{r}_1$ and travels across the wire along the two cyclotron orbits. The pair of the quasiparticle waves in the two branches are reflected again into the two branches at $\mathbf{r}_2$. After the two reflections, the incident quasiparticle divides into four parts. The two parts in the electron (hole) branch interfere with each other. During the trip between $\mathbf{r}_1$ and $\mathbf{r}_2$, the quasiparticle in the electron (hole) branch suffers the phase change ϕ_B^e (ϕ_B^h) from the vector potential. It was shown that the phase difference between the pair of the waves $\phi_B^e-\phi_B^h$ is $2\pi\mu_N/\hbar\omega_c$, which is independent of the incident angle of the electronlike quasiparticle. The phase difference $2\pi\mu_N/\hbar\omega_c$ is not proportional to the magnetic flux enclosed by the two partial circles between $\mathbf{r}_1$ and $\mathbf{r}_2$ but the magnetic flux encircled by the single complete cyclotron orbit in units of $\phi_0\equiv 2\pi\hbar c/|e|$.[12] This is because the phase shift is proportional to the charge of the quasiparticle and the signs of the charge in the two branches are opposite to each other. Thus the Aharonov-Bohm type oscillations can be seen in the magnetoconductance. (The Aharonov-Bohm effect is the interference effect of an electron *in the absence of the magnetic field*.[19] In this paper, however, we use the term ''Aharonov-Bohm type interference effect'' when we explain the mechanism of the conductance oscillations, which is the interference effect *in the presence of the magnetic field*.)

Based on the above idea, we derived the zero-bias differential conductance

$$G\sim\frac{2e^2}{h}N_c\Big[1-(|r^{ee}|^2-|r^{he}|^2)^2 -4|r^{ee}|^2|r^{he}|^2 p\left(\frac{\mu_N}{\hbar\omega_c}\right)^2\cos\left(2\pi\frac{\mu_N}{\hbar\omega_c}-2\,\theta_n\right)\Big], \tag{2.2}$$

where $|r^{ee}|^2$ ($|r^{he}|^2$) is the normal (Andreev) reflection probability, θ_n is the phase shift of the normal reflection, N_c is the number of the propagating channels in the semiconductor, and $p(\mu_N/\hbar\omega_c)=2(1-L_C/W)$ is the envelope function given by the phenomenological argument, respectively.[12] Note, however, that the sign of the last term in Eq. (2.2) had to be adjusted by hand, from $+$ to $-$, in order to obtain agreement with the numerical results.

The conductance expression is valid when the magnetic field satisfies a relation

$$\frac{W}{2}\leqslant L_C\leqslant W, \tag{2.3}$$

where the incident quasiparticle is reflected twice at the Sm-S interface. In the absence of the disorder in the Sm-S junction, the analytic expression well explains the amplitude, the period, and the phase shift of the conductance oscillations.[12,13] Thus we concluded that the Aharonov-Bohm type interference effect of a quasiparticle is responsible for the conductance oscillations even in the simply connected Sm-S junctions. In general, in order to observe the Aharonov-Bohm type conductance oscillations clearly, we have to confine an electron wave as in the experiment[20] and/or the magnetic flux as in the original idea.[19] An electron wave in the ballistic transport regime, however, is confined within the cyclotron orbit by its charge degree of freedom under sufficiently strong magnetic fields.[21,22]

If the above physical picture of the conductance oscillations is correct, the oscillations are sensitive to imperfections near the Sm-S interface since the quasiparticle in the present system is confined only by the magnetic field. In order to find the conductance oscillations, the quasiparticle must skip between $\mathbf{r}_1$ and $\mathbf{r}_2$ in Fig. 1(b) without being scattered by the impurities. In other words, the mean-free-path in the semiconductor, l, must be larger than the mean orbit length of the cyclotron motion between the two reflection points $\pi L_C/2$. In addition to this, the conductance oscillations require the specular reflection of the quasiparticle at the Sm-S interface. In the presence of the roughness at the interface, there will be the ''diffuse'' reflection. The pair of the waves that suffer the diffuse reflection at $\mathbf{r}_1$ cannot meet each other again at $\mathbf{r}_2$. In real Sm-S junctions, however, the disorder exists near the Sm-S interface and may suppress the conductance oscillations.[23]

III. EFFECTS OF DISORDER

The Sm-S junction is described by the Bogoliubov-de Gennes equation[24] on the two-dimensional tight-binding model as shown in Fig. 2(a), where j labels the lattice site in the x direction. The lattice sites for $j\leqslant 0$ and $j\geqslant 1$ represent the semiconductor and the superconductor, respectively. The vector potential is chosen to be $\mathbf{A}=(0,Bx)$ in the semicon-

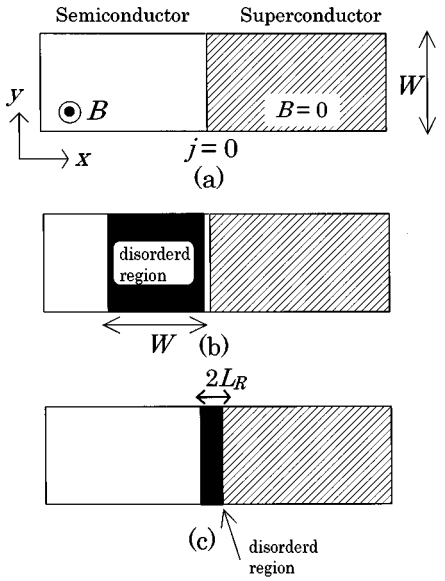

FIG. 2. The Sm-*S* junction is illustrated. The hatched area denotes the superconductor. We introduce the square shaped disordered region (filled area) near the interface in (b). The disordered region is limited at the interface in (c).

ductor and zero in the superconductor, respectively. We use the hard wall confinement potential in the *y* direction and the lattice index in this direction is *m*. The Bogoliubov-de Gennes equation reads

$$\begin{pmatrix} \hat{h}_0 & \hat{\Delta} \\ \hat{\Delta}* & -\hat{h}_0^* \end{pmatrix} \mathbf{f}(j',m') = E\mathbf{f}(j',m'), \tag{3.1}$$

with

$$\hat{h}_0 = \sum_{j,m} (-t_j|j,m\rangle\langle j+1,m| + \text{H.c.}) + \sum_{j,m} (-t_j e^{ih_B j}|j,m+1\rangle \times \langle j,m| + \text{H.c.}) + \sum_{j,m} E_{i,j}|j,m\rangle\langle j,m|, \tag{3.2}$$

$$\hat{\Delta} = \sum_{j,m} \Delta_{j,m}|j,m\rangle\langle j,m|, \tag{3.3}$$

$$\mathbf{f}(j,m) = \begin{pmatrix} u_{j,m}|j,m\rangle \\ v_{j,m}|j,m\rangle \end{pmatrix}, \tag{3.4}$$

where $E_{j,m} = \epsilon_{j,m} + 4t_j - \mu_j$ corresponds to the on-site potential and $\epsilon_{j,m}$ is the random potential. The hopping integral and the Fermi energy are $t_j = t_N$ and $\mu_j = \mu_N$ in the semiconductor ($j \leqslant 0$) and those in the superconductor ($j \geqslant 1$) are $t_j = t_S$ and $\mu_j = \mu_S$, respectively. The hopping integral gives the bandwidth and the Fermi energy corresponds to the difference in energy between the band edge and the chemical potential of the Sm-*S* junction. We note that the chemical potential of the Sm-*S* junction is set to be the origin of the energy. The pair potential $\Delta_{j,m}$ is Δ_0 in the superconductor and zero in the semiconductor, respectively. The amplitude of the wave function in the electron (hole) branch is $u_{j,m}$ ($v_{j,m}$). The magnetic field is taken into account through the Peierls phase $h_B = 2\pi Ba^2/\phi_0$ in the hopping Hamiltonian,

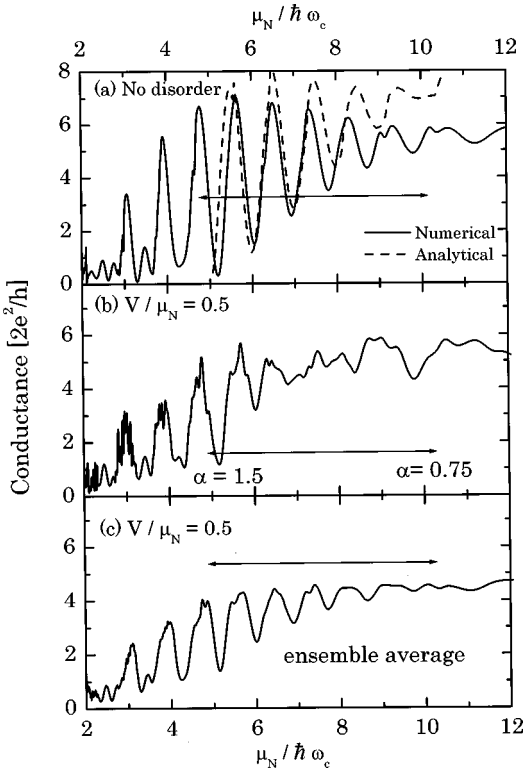

FIG. 3. The conductance is plotted as a function of the inverse of the magnetic field, where $t_N/\mu_N = 0.5$, $t_S/\mu_N = 1.5$, and $\mu_S/\mu_N = 2.0$, respectively. The width of the Sm-*S* junction *W* is 30 lattice constant. We do not consider any disorder in (a) and compare the analytic results in Eq. (2.2) (broken line) with the numerical results (solid line). The range of the magnetic field, $W/2 < L_C < W$, is denoted by $\leftrightarrow$. In (b), we introduce the square shaped disordered region as shown in Fig. 2(b), where $V/\mu_N = 0.5$. The parameter $\alpha = l/(\pi L_C/2)$ is the ratio of the elastic mean-free-path in 2DEG and the mean orbit length of the cyclotron motion. The ensemble-averaged conductance for $V/\mu_N = 0.5$ is shown in (c).

where *a* is the lattice constant. In what follows, the energy is measured in units of μ_N and the length is measured in units of the lattice constant. We fix the parameters as $t_N/\mu_N = 0.5$, $\mu_S/\mu_N = 2.0$, and $\Delta_0/\mu_N = 0.005$, respectively. The width of the junction is 30 lattice constant. We numerically calculate the reflection probability by using the recursive Green's-function method[16,17] and obtain the zero-bias differential conductance based on the Takane-Ebisawa formula.[18]

A. Disorder in Semiconductor

In Fig. 3(a), we show the conductance as a function of $\mu_N/\hbar\omega_c$, where $t_S/\mu_N = 1.5$. The range of the magnetic field, which satisfies Eq. (2.3), is denoted by $\leftrightarrow$. Here there is no disorder in the Sm-*S* junction. The analytic expression in Eq. (2.2) (broken line) is compared with the numerical results (solid line), where we estimate $|r^{ee}|^2$ and $|r^{he}|^2$ from the numerical results at $B = 0$ and θ_n is set to be zero. The analytic results agree well with the numerical results.

We introduce the square shaped disordered region in the semiconductor as shown in Fig. 2(b), where the on-site potential is given randomly in the range of $-V/2 < \epsilon_{j,m} < V/2$, which represents the impurity potential. The disordered region is separated by $W/10$ from the interface in order to

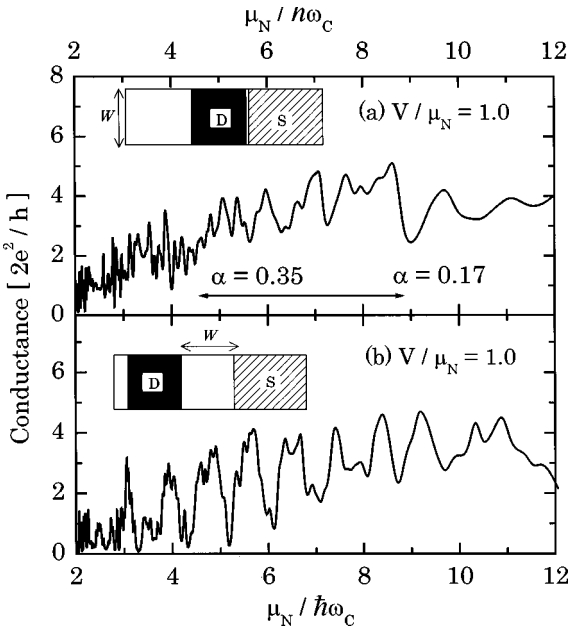

FIG. 4. We compare the conductance in the two systems in (a) and (b), where $V/\mu_N=1.0$. In insets, the filled area denoted by D is the disordered region. In (a), the disordered region is introduced near the interface. On the other hand in (b), the disordered region is separated by W from the interface.

neglect the effects of the rough interface, which will be discussed in the next subsection. In Fig. 3(b), we show the conductance for $V/\mu_N=0.5$. The parameter α is the ratio of the elastic mean-free-path l and the mean orbit length of the cyclotron motion between the two reflection points at the interface $\pi L_C/2$, [i.e., $\alpha \equiv l/(\pi L_C/2)$]. Since the diameter of the cyclotron orbit depends on the magnetic field, α is shown at the both edges of Eq. (2.3). The elastic mean-free-path is estimated from the normal conductance of the disordered region. The conductance oscillations cannot be seen around $\mu_N/\hbar\omega_c \sim 10$ because the impurity scattering suppresses the interference effect (i.e., $\alpha<1.0$). On the other hand for $\mu_N/\hbar\omega_c \sim 5$, the oscillations still can be seen because the mean orbit length is slightly smaller than l. The calculated results are consistent with the prediction in Sec. II. We conclude that l must be larger than $\pi L_C/2$ to observe the conductance oscillations.

The disorder in the semiconductor suppresses the conductance oscillations in the two different mechanisms. The impurity scattering suppresses the interference effect as discussed in Fig. 3(b). The disordered segment causes the backscattering of an incoming quasiparticle before it reaches at the Sm-S interface, which also leads to the suppression of the conductance oscillations. Actually the amplitudes of the conductance and the conductance oscillations in Fig. 3(b) decrease in comparison with those in Fig. 3(a). In order to separate the two effects clearly, we examine the conductance in the two different systems as shown in Figs. 4(a) and 4(b), where $V/\mu_N=1.0$. In Fig. 4(a), the square shaped disordered region is introduced near the interface as shown in the inset. On the other hand in Fig. 4(b), the disordered segment is separated by W from the interface as shown in the inset. The amplitude of the incident quasiparticle reaching at the interface is decreased due to the backscattering in the disordered region in both Figs. 4(a) and 4(b). In Fig. 4(a), the Aharonov-Bohm type oscillations are completely smeared by the impurity scattering near the interface because $\alpha<1.0$ holds for all magnetic fields. The aperiodic oscillations of the universal conductance fluctuations[25–28] can be seen instead of the Aharonov-Bohm type oscillations. In Fig. 4(b), the small aperiodic oscillations are caused by introducing the disordered segment but the periodic oscillations still can be seen in the conductance. In this case, the Aharonov-Bohm type oscillations remain because there is no impurities near the interface. The calculated results in Fig. 4 support the proposed mechanism of the conductance oscillations.

We have shown the conductance of a single sample with a particular random arrangement of the on-site potentials in Fig. 3(b). In Fig. 3(c), we show the conductance averaged over 20 different random configurations for $V/\mu_N=0.5$. In comparison with Fig. 3(b), the conductance oscillations seem to be recovered even if $\alpha<1.0$ because the aperiodic oscillations of the magnetofinger print are averaged out. It may be difficult to observe the ensemble-averaged conductance in experiments, however, Fig. 3(c) implies the difference in the characteristic behavior between the Aharonov-Bohm type oscillations and the magnetofinger print. In the real three-terminal junctions, the Fermi energy in 2DEG can be changed by the gate voltage.[29] It may be possible to find the oscillations in the ensemble-averaged conductance by tuning the Fermi energy.

B. Roughness at the interface

We introduce disorder on the $2L_R \times W$ lattice sites that satisfy $-L_R+1 \leqslant j \leqslant L_R$ as shown in Fig. 2(c). The rough interface is represented by changing the on-site potential ($E_{j,m}$) and the pair potential ($\Delta_{j,m}$). In the absence of the roughness, the potentials in the semiconductor are $E_{j,m}=4t_N-\mu_N$ and $\Delta_{j,m}=0$, respectively. In the presence of the roughness, these potentials on the lattice sites for $-L_R+1 \leqslant j \leqslant 0$ are replaced by $E_{j,m}=4t_S-\mu_S$ and $\Delta_{j,m}=\Delta_0$ with a probability p_R. In the same way, the potentials on the lattice sites for $1 \leqslant j \leqslant L_R$ are replaced by $E_{j,m}=4t_N-\mu_N$ and $\Delta_{j,m}=0$ with a probability p_R. In this model, $p_R \leqslant 0.5$ and $L_R \ll W$ represent the degree of disorder. The random on-site potential $\epsilon_{j,m}$ is fixed at zero. In Fig. 5, we show the numerical results of the conductance (solid line) for three choices of p_R and L_R, where $t_S/\mu_N=1.0$.

The roughness at the interface suppresses the conductance oscillations in the two different mechanisms. The specular reflection is suppressed by the roughness as discussed in Sec. II. In addition to this, the Andreev reflection probability is also decreased by the roughness at the interface. In order to consider the two effects separately, we modify the expression of the conductance,

$$G \sim \frac{2e^2}{h} N_c \Bigg[1-(\langle |r^{ee}|^2-|r^{he}|^2\rangle)^2-4\langle |r^{ee}|^2\rangle\langle |r^{he}|^2\rangle\langle s^{ee}\rangle \times\langle s^{he}\rangle p\left(\frac{\mu_N}{\hbar\omega_c}\right)^2 \cos\left(2\pi\frac{\mu_N}{\hbar\omega_c}-2\theta_n\right)\Bigg], \tag{3.5}$$

where $\langle\cdots\rangle$ means the ensemble-average value at $B=0$ and s^{ee} (s^{he}) is the specularity parameter for the normal (An-

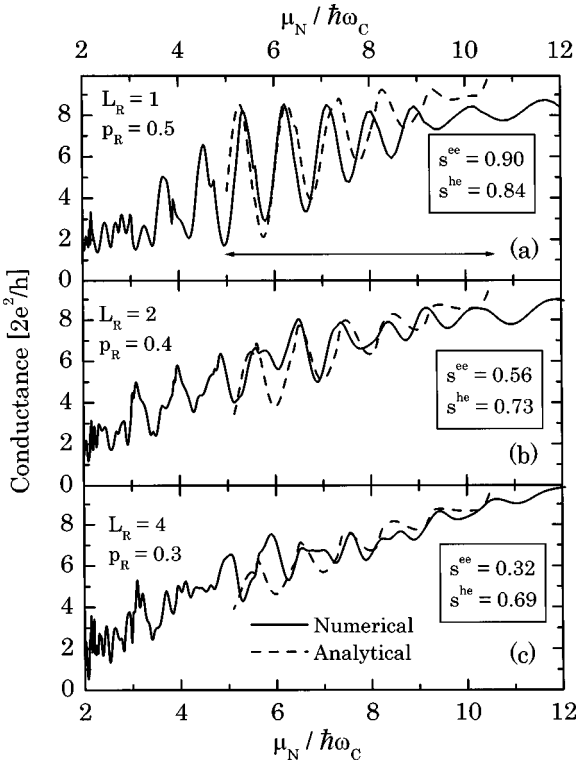

FIG. 5. The conductance in the presence of the roughness at the interface is shown. The solid lines are the numerical results and the broken lines are the analytic results in Eq. (3.5), respectively. In (a)–(c), the reflection probabilities are $\langle|r^{ee}|^2\rangle \sim 0.73$ and $\langle|r^{he}|^2\rangle \sim 0.27$ as shown in the Table I. The range of the magnetic field that satisfies $W/2 < L_C < W$ is denoted by $\leftrightarrow$.

dreev) reflection. Under the periodic boundary condition in the y direction and $B=0$, we calculate the ensemble-averaged values as follows,

$$\langle|r^{ee}|^2\rangle = \left\langle \sum_{l,l'} |r^{ee}_{l',l}|^2 \right\rangle \Big/ N_c, \tag{3.6}$$

$$\langle|r^{he}|^2\rangle = \left\langle \sum_{l,l'} |r^{he}_{l',l}|^2 \right\rangle \Big/ N_c, \tag{3.7}$$

$$\langle s^{ee}\rangle = \left\langle \sum_{l} |r^{ee}_{l,l}|^2 \right\rangle \Big/ N_c\langle|r^{ee}|^2\rangle, \tag{3.8}$$

$$\langle s^{he}\rangle = \left\langle \sum_{l,\tilde{l}} |r^{he}_{\tilde{l},l}|^2 \right\rangle \Big/ N_c\langle|r^{he}|^2\rangle. \tag{3.9}$$

The summation $\Sigma_{l,l'}$ runs over all propagating channels in the semiconductor and $r^{ee}_{l',l}$ ($r^{he}_{l',l}$) is the reflection coefficient from the lth propagating channel in the electron branch to the l'th channel in the electron (hole) branch. The signs of the all velocity components in the hole channel denoted by $\tilde{l}$ are opposite to those in the incoming electron channel labeled by l. In the absence of the roughness, the perfect specular reflection is represented by $\langle s^{ee}\rangle = \langle s^{he}\rangle = 1$. In Eq. (3.5), the specularity of the Sm-S interface is considered through $\langle s^{ee}\rangle$ and $\langle s^{he}\rangle$.

TABLE I. Values of $\langle r^{ee}\rangle$, $\langle r^{he}\rangle$, $\langle s^{ee}\rangle$, and $\langle s^{he}\rangle$ used in Eq. (3.5) and in Fig. 4. These are the ensemble-averaged values over a number of random configurations at $B=0$.

	L_R	P_R	$\langle\|r^{ee}\|^2\rangle$	$\langle\|r^{he}\|^2\rangle$	$\langle s^{ee}\rangle$	$\langle s^{he}\rangle$
	0	0.0	0.46	0.54	1.00	1.00
(a)	1	0.5	0.72	0.28	0.90	0.84
(b)	2	0.4	0.74	0.26	0.56	0.73
(c)	4	0.3	0.73	0.27	0.32	0.69

In Fig. 5, we compare the analytic results in Eq. (3.5) (broken line) with the numerical results. In Table I, we summarize the reflection probabilities and the specularity parameters used in Eq. (3.5). We note that $\langle|r^{ee}|^2\rangle$ ($\langle|r^{he}|^2\rangle$) has almost the same value in the three choices of (p_R, L_R). Thus the difference in the amplitude of the oscillations among Figs. 5(a)–5(c) is stemming from the specularity of the interface. The analytic expression agrees well with the all numerical results. The amplitude of the oscillations decreases with decreasing specularity parameters, which indicates that the specular reflection at the Sm-S interface is an important ingredient for the conductance oscillations.

We have calculated the specularity parameters for $0 < p_R \leq 0.5$ and $1 \leq L_R \leq 4$. Within our numerical results, we find an interesting feature in $\langle s^{ee}\rangle$ and $\langle s^{he}\rangle$. The specularity parameter in the Andreev reflection tends to be larger than that in the normal reflection for many cases. We cannot give a convincing argument, however, one explanation for this fact is as follows. The specularity parameters are estimated in the absence of the magnetic field. The retro property of the quasiparticle holds in the presence of the time-reversal symmetry. The Andreev-reflected holelike quasiparticle may tend to trace back the trajectory of the incoming electronlike quasiparticle even if the roughness exists at the interface. In addition to this, $\langle s^{ee}\rangle$ tends to first decrease then increase with increasing roughness for large L_R. We find that a relation $\langle s^{ee}\rangle\langle s^{he}\rangle > 0.2$ holds for all cases. In Eq. (3.5), the amplitude of the conductance oscillations is proportional to $\langle|r^{ee}|^2\rangle\langle|r^{he}|^2\rangle$ and $\langle s^{ee}\rangle\langle s^{he}\rangle$. Since $\langle s^{he}\rangle$ remains with large values, roughly speaking, a relation

$$\langle|r^{ee}|^2\rangle\langle|r^{he}|^2\rangle \leq \langle s^{ee}\rangle\langle s^{he}\rangle \tag{3.10}$$

holds for many cases. The relation in Eq. (3.10) implies that the reflection at the Sm-S interface is sufficiently specular when the Andreev reflection probability is sufficiently large. In this paper, we have considered the suppression of the Andreev reflection and the suppression of the specular reflection independently. The two effects, however, are closely related to each other.

IV. DISCUSSION

The perfect screening of the magnetic field in the superconductor has been assumed in the theoretical works.[11,12,14] The phenomenological theory predicted that the penetration depth of the superconductor λ must be smaller than W to find the conductance oscillations.[13] This argument is briefly summarized as follows. At $\mathbf{r}_1$ in Fig. 1(b), the incident quasiparticle can penetrate into the superconductor within the length

scale given by $\xi_0=\hbar v_S/\pi\Delta_0$ and can move to $\mathbf{r}_2$ through the superconductor, where v_S is the Fermi velocity in the superconductor. When the magnetic field penetrates into the superconductor, the quasiparticle reaching at $\mathbf{r}_2$ suffers the phase change that is roughly estimated as $\phi_B^S=eB\lambda W/\hbar c$. This phase shift, however, smears the conductance oscillations because the quasiparticle is not confined within a particular propagation path in the superconductor. When λ is much smaller than W, so that $\phi_B^S \ll 2\pi\mu_N/\hbar\omega_c$, the conductance oscillations can be seen. From the equations $\phi_B^S < 2\pi\mu_N/\hbar\omega_c$, Eqs. (2.3) and (2.1), a condition $\lambda/W < 0.03\sim 0.1$ must be satisfied to observe the conductance oscillations. Actually we have confirmed by the numerical simulation that the oscillations are clearly seen for $\lambda/W < 0.05$ and disappear for $\lambda/W > 0.1$.

From the numerical results in Sec. III, we derive an important relation to find the conductance oscillations. The mean-free-path in the semiconductor is larger than the mean orbit length of the cyclotron motion, i.e., $l/(\pi L_C/2) > 1$. The width of the junction must be much larger than the penetration depth in the superconductor, i.e., $\lambda/W \leqslant 0.05$. In addition to these conditions, the magnetic field is strong enough to satisfy Eq. (2.3), and the superconductivity holds. A relation

$$l > W \sim L_C \gg \lambda \tag{4.1}$$

must be satisfied to find the conductance oscillations in experiments. The mean-free-path in a real S-Sm-S junction is about $l\sim 0.8$ μm in 2DEG on InAs.[7] However, l can be more than 10 μm on GaAs. In the following, we assume that $W \sim 10$ μm. In this case, the penetration depth in the superconductor is much smaller than W since λ is typically 0.1 μm. The magnetic field in Eq. (2.3) is estimated to be $0.08\ \mathrm{T} > B > 0.04\ \mathrm{T}$. Here we use the parameters such as $\mu_N = 100$ meV and $m^* = 0.05 m_e$, where m_e is the bare mass of an electron. The critical magnetic field of the type I superconductor can be larger than 0.04 T in materials such as Pb. Thus it seems to be possible to fabricate the Sm-S junctions that satisfy the relation in Eq. (4.1).

V. CONCLUSION

The magnetoconductance oscillations in a semiconductor/superconductor (Sm-S) junction were shown in a numerical simulation.[11] In experiments, however, the conductance oscillations have never been observed yet. In previous papers,[12,13] we proposed the mechanism of the conductance oscillations and concluded that the oscillations are a consequence of the Aharonov-Bohm type interference effect. If the proposed mechanism is correct, it was predicted that the conductance oscillations would be sensitive to the disorder near the Sm-S interface and to the magnetic field penetration into the superconductor.[13] In this paper, we perform a numerical simulation by using the recursive Green's-function method in order to confirm the prediction. The numerical results show that the conductance oscillations are suppressed by the disorder near the interface. The calculated results agree well with the prediction even quantitatively, which indicates the justification of the proposed mechanism of the conductance oscillations. We also discuss a possibility of the conductance oscillations in experiments.

ACKNOWLEDGMENTS

The authors are indebted to N. Tokuda and H. Akera for useful discussion. The computations have been carried out at the Supercomputer Center, Institute for Solid State Physics, University of Tokyo.

*Email: asano@eng.hokudai.ac.jp

[1] B.J. van Wees and H. Takayanagi, in *Mesoscopic Electron Transport*, edited by L.L. Sohn, L.P. Kouwenhoven, and G. Schön, NATO ASI Series (Kluwer Academic, Dordrecht, 1996).
[2] C.W.J. Beenakker, Rev. Mod. Phys. **69**, 731 (1997), and references therein.
[3] A.F. Morpurgo, S. Holl, B.J. van Wees, T.M. Klapwijk, and G. Borghs, Phys. Rev. Lett. **78**, 2636 (1997).
[4] G. Bastian, E.O. Göbel, A.B. Zorin, H. Schlze, J. Niemeyer, T. Weimann, M.R. Benett, and K.E. Singer, Phys. Rev. Lett. **81**, 1686 (1998).
[5] A.F. Andreev, Zh. Éksp. Theor. Fiz. **46**, 1823 (1964) [Sov. Phys. JETP **19**, 1228 (1964)].
[6] G.E. Blonder, M. Tinkham, and T.M. Klapwijk, Phys. Rev. B **25**, 4515 (1982).
[7] H. Takayanagi and T. Akazaki, Physica B **249-251**, 462 (1998).
[8] T.D. Moore and D.A. Williams, Phys. Rev. B **59**, 7308 (1999).
[9] A.Yu. Zyuzin, Phys. Rev. B **50**, 323 (1994).
[10] Y. Ishikawa and H. Fukuyama, J. Phys. Soc. Jpn. **68**, 954 (1999).
[11] Y. Takagaki, Phys. Rev. B **57**, 4009 (1998).
[12] Y. Asano, Phys. Rev. B **61**, 1732 (2000).
[13] Y. Asano and T. Kato, J. Phys. Soc. Jpn. (to be published).
[14] H. Hoppe, U. Zülicke, and G. Schön, Phys. Rev. Lett. **84**, 1804 (2000).
[15] Y. Takagaki and K.H. Ploog, Phys. Rev. B **58**, 7162 (1998).
[16] P.A. Lee and D.S. Fisher, Phys. Rev. Lett. **47**, 882 (1981).
[17] T. Ando, Phys. Rev. B **44**, 8017 (1991).
[18] Y. Takane and H. Ebisawa, J. Phys. Soc. Jpn. **61**, 1685 (1992).
[19] Y. Aharonov and D. Bohm, Phys. Rev. **115**, 485 (1959).
[20] R.A. Webb, S. Washburn, C.P. Umbach, and R.B. Laibowitz, Phys. Rev. Lett. **54**, 2696 (1985).
[21] H. van Houten, B.J. van Wees, J.E. Mooij, C.W.J. Beenakker, J.G. Williamson, and C.T. Foxon, Europhys. Lett. **5**, 721 (1988).
[22] P.A.M. Benistant, H. van Kempen, and P. Wyder, Phys. Rev. Lett. **51**, 817 (1983).
[23] F.W.J. Hekking and Yu.V. Nazarov, Phys. Rev. Lett. **71**, 1625 (1993).
[24] P.G. de Gennes, *Superconductivity of Metals and Alloys* (Benjamin, New York, 1966).
[25] P.A. Lee and A.D. Stone, Phys. Rev. Lett. **55**, 1622 (1985).
[26] B.L. Al'tshuler, Pis'ma Zh. Éksp. Teor. Fiz. **41**, 530 (1985) [JETP Lett. **41**, 648 (1985)].
[27] I.K. Marmorkos, C.W.J. Beenakker, and R.A. Jalabert, Phys. Rev. B **48**, 2811 (1993).
[28] P.W. Brouwer and C.W.J. Beenakker, Phys. Rev. B **52**, 16 772 (1995).
[29] H. Takayanagi, J. Bindslev, and J. Nitta, Phys. Rev. Lett. **74**, 166 (1995).